Research Article

Received: 1 July 2019 Revised: 18 October 2019 Accepted article published: 19 November 2019 Published online in Wiley Online Library: 20 December 2019

(wileyonlinelibrary.com) DOI 10.1002/pi.5942

Synthesis and electropolymerization of a multifunctional naphthalimide clicked carbazole derivative

Fatma Coban,[a] Rukiye Ayranci[b] and Metin Ak[c]*

Abstract

In this study, a multifunctional 'clicked' naphthalimide carbazole derivative (CNaP) was synthesized via Huisgen 1,3-dipolar cycloaddition reaction. Combining carbazole as an electroactive group with naphthalimide as a fluorescence group via click chemistry imparts multifunctional properties to this unique structure. CNaP was characterized via Fourier transform IR, ^{13}C and ^{1}H NMR spectroscopy as well as fluorescence and electrochemical measurements. The electrochemical polymerization of the CNaP monomer was carried out in acetonitrile/boron trifluoride diethyl etherate (2:1) (v/v) by the cyclic voltammetry technique. The resulting polycarbazole-derived conductive polymer was characterized via optical and electrochemical measurements. PCNaP displayed multi-electrochromism behaviour with good optical contrast (41% at 693 nm) and switching time (1.92 s at 693 nm). These results demonstrate that the new 'clicked' fluorescent, polycarbazole-derived conductive polymer can be used in various applications such as electrochemical/optical sensors and electrochromic and fluorescence imaging devices.

Keywords: carbazole; 1,8-naphthalimide; click chemistry; semiconducting polymer; electrochemistry

INTRODUCTION

Semiconducting polymers have attracted remarkable attention due to their wide range of applications such as organic light-emitting diodes,[1–3] smart windows,[4–10] sensors[11–19] and photovoltaic cells.[20–23] Recent advances in industrial research require the design and synthesis of new multifunctional semiconducting polymers.[24–26] Carbazole derivatives have a potential use in optoelectronic devices due to their easy functionalization, thermal/photochemical stability and photoconductive and electroluminescent properties.[27–30]

1,8-Naphthalimide derivatives have been reported to be used in a variety of applications due to their strong electroactivity, fluorescence and photostability.[31] They have been used in many fields such as fluorescent sensors, switchers and electroluminescent material.[32] They have also been used as fluorescent markers and molecular probes in biotechnology and as sensitive electro-optic materials in solar cells and organic field-effect transistors.[33–35]

The Cu(I)-catalyzed 1,3-dipolar azide-alkyne cycloaddition reaction called 'click chemistry' which was discovered by Sharpless and Torneo in 2001 has recently been one of the most interesting research topics for obtaining multifunctional materials.[36] Thanks to its impressive robustness, such as high efficiency, functionality tolerance, high reaction rate, simple reaction conditions and selectivity, the click reaction protocol has been widely used to synthesize dendrimer structures, nanoparticles, semiconducting polymers and to modify natural products and the surfaces of thin films.[37–43] This contribution of cyclization will allow the creation of interesting syntheses to form multifunctional materials with easy tools, rather than the previously long and difficult methods.[44] Click chemistry can be a good alternative synthetic path to produce multifunctional semiconducting polymers without having to employ expensive and complicated reaction conditions. Therefore, in this study, the click reaction was specifically chosen because of the simplicity of the reaction of terminal alkynes and azides in carbazole that is electroactive with a naphthalimide group that has fluorescent properties.

A new multifunctional monomer 2-((9H-carbazol-2-yl)oxy)-*N*-((1-(4-(1,3-dioxo-1H-benzo[de]-isoquinolin-2(3H)-yl)phenyl)-1H-1,2,3-triazol-4-yl)methyl)acetamide (CNaP) was synthesized via the click reaction of 2-((9H-carbazol-2-yl)oxy)-*N*-(prop-2-yn-1-yl) acetamide (**3**) and 2-(4-azido-phenyl)-1H-benzo[de]iso-quinoline-1,3(2H)-dion (NaP). Thereafter its chemical structure was characterized by ^{1}H NMR, ^{13}C NMR spectroscopy and the Fourier transform IR (FTIR) technique; CNaP monomer was electrochemically polymerized, and the optical and electrical properties of the resulting semiconducting polymer were characterized by spectro-electrochemical techniques. These results indicate that both CNaP and its polymer have potential for important applications in the field of electrochemical/optical sensors, electrochromic devices and fluorescence imaging applications.

* *Correspondence to: M Ak, Department of Chemistry, Pamukkale University, 20020 Denizli, Turkey. E-mail: metinak@pau.edu.tr*

a *Chemistry Department, Faculty of Art and Science, Burdur Mehmet Akif Ersoy University, Burdur, Turkey*

b *Simav Vocational High School, Laboratory Technology Program, Kutahya Dumlupinar University, Kutahya, Turkey*

c *Chemistry Department, Faculty of Art and Science, Pamukkale University, Denizli, Turkey*

EXPERIMENTAL

Materials

Propargylamine, chloroacetyl chloride, boron trifluoride diethyl etherate (BFEE), 1,8-naphthalic anhydride, *p*-phenylenediamine, sodium bicarbonate, sodium iodide, potassium carbonate, hydrochloric acid, sodium nitrite, sodium azide, copper(II) sulfate pentahydrate, (+)-sodium L-ascorbate, *N*,*N*-dimethylformamide, dichloromethane (DCM), acetonitrile (ACN), acetone, ethyl acetate and tetrahydrofuran were acquired from Sigma Aldrich (St. Louis, MO, USA). 2-Hydroxycarbazole and magnesium sulfate was purchased from Alfa Aesar (Kandel Germany) and Pub-Chem (Bethesda, MD, USA), respectively, and were used without any purification.

Instrumentation

Electrochemical characterization and the spectroelectrochemical properties of the semiconducting polymers were analyzed with an Ivium potentiostat/galvanostat and Agilent 8453 UV–visible spectrophotometer. All compounds were characterized by ^{1}H NMR, ^{13}C NMR (a Varian 400 MHz spectrometer), an FTIR spectrophotometer (Perkin-Elmer 2000) and a fluorescence spectrophotometer (Agilent Cary Eclipse). All measurements were performed at room temperature.

Synthesis CNaP monomer

*2-Iodo-*N*-(prop-2-yn-1-yl)acetamide (**2**)*

The reaction route is shown in Scheme 1. 2-Chloro-*N*-(prop-2-yn-1-yl)acetamide (**1**) was synthesized according to the published literature procedure.[45] Compound **1** (1.32 g, 10 mmol) and NaI (3 g, 20 mmol) in acetone (25 mL) were refluxed for 7 h. At the end of this time, the acetone evaporated. The resulting product was crystallized from ethyl acetate to give the product as white crystals (1.2 g), yield 54%. Melting point 112–115 °C. IR (cm^{-1}): 3282 (stretching N—H), 3268 (alkyne C—H), 2968 (alkane C—H), 1639 (amide C=O), 1544 (bending N—H), 1424, 1363, 1272, 1159, 1031, 927, 881.

*2-((9H-carbazol-2-yl)oxy)-*N*-(prop-2-yn-1-yl)acetamide (**3**)*

2-Hydroxycarbazole (0.73 g, 4 mmol), propargyl iodine (**2**) (1.12 g, 5 mmol) and K_2CO_3 (1.65 g, 12 mmol) were refluxed in ACN (40 mL) for 4 days. Water was added to the reaction mixture and filtered to obtain an off-white solid (0.9 g), yield 81%. Melting point 177–178 °C. IR (cm^{-1}): 3394 (stretching N—H), 3243 (alkyne C≡C—H), 3050 (aromatic C—H), 2890 (aliphatic C—H), 2120 (alkyne C≡C), 1667 (amide C=O), 1607 (bending N—H), 1580, 1494, 1463, 1313, 1293, 1181, 1069, 1028, 961, 872. ^{1}H NMR (400 MHz, deuterated dimethylsulfoxide (DMSO-d_6)): δ 11.13 (1H (N—H), br, s); 8.59 (1H (N—H), br, s); 7.94 (2H, d); 7.37 (1H, d); 7.26 (1H, t); 7.06 (1H, t); 6.96 (1H, s); 6.80 (1H, d); 4.56 (2H, s); 3.91 (2H, d); 3.07 (1H, s).

*2-(4-Azidophenyl)-1H-benzo[de]isoquinoline-1,3(2H)-dione (**5**)*

The synthesis of 2-(4-aminophenyl)-1H-benzo[de]isoquinoline-1, 3(2H)-dione (**4**) was carried out according to the literature.[46] 4 mL of 15% HCl were added to **4** (1 g, 3.47 mmol) at 0 °C. $NaNO_2$ (0.48 g, 6.94 mmol) in 8 mL of water was slowly added to the reaction mixture at 0 °C. After stirring for 30 min at 0 °C, NaN_3 (0.56 g, 8.68 mmol) in water (4 mL) was added dropwise and stirred for 2 h at 0 °C. The solid was precipitated by adding water. A white solid was obtained (0.73 g), yield 67%. Melting point 208–209 °C. IR (cm^{-1}): 3067 (aromatic C—H), 2108 (azide N_3), 1659 (C=O), 1624, 1506, 1434, 1372, 1356, 1234, 1121, 1025, 949, 830. ^{1}H NMR (400 MHz, DMSO-d_6): δ 8.46 (4H, dd); 7.87 (2H, t); 7.39 (2H, d); 7.24 (2H, d).

*2-((9H-carbazol-2-yl)oxy)-*N*-((1-(4-(1,3-dioxo-1H-benzo[de] isoquinolin-2(3H)-yl)phenyl)-1H-1,2,3-triazol-5-yl)methyl) acetamide (CNaP)*

Compounds **3** (0.28 g, 1 mmol) and **5** (0,31 g, 1 mmol) were dissolved in tetrahydrofuran/H_2O (4/1 (v/v), 24 mL); aqueous $CuSO_4.5H_2O$ (5.3 mg, 0.021 mmol) and sodium ascorbate (0.02 g, 0.10 mmol) were added, and the reaction mixture was stirred at 85 °C overnight. The precipitate was filtered and washed with water to give a yellow solid (0.45 g), yield 76%. Melting point 262–263 °C. IR (cm^{-1}): 3288 (stretching N—H), 3142 (triazole C—H), 3068 (aromatic C—H), 2963 (aliphatic C—H), 1705 (anhydride C=O), 1660 (amide C=O), 1608 (bending N—H), 1587 (bending C—H), 1519, 1484, 1375, 1314, 1236, 1171, 1048, 992, 778. ^{1}H NMR (400 MHz, DMSO-d_6): δ 11.14 (1H (N—H), br, s); 8.79 (1H (N—H), br, s); 7.56 (1H (triazole, s); 8.51–6.87 (19H, Ar–CH); 4.24 (4H, s). ^{13}C NMR (400 MHz, DMSO-d_6): δ = 168.5, 164.0, 163.4, 157.2, 146.7, 141.3, 140.2, 136.7, 136.5, 135.0, 131.9, 131.2, 128.7, 128.3, 127.7, 124.7, 123.0, 121.3, 120.9, 119.8, 119.0, 118.9, 117.2, 111.1, 108.5, 96.2, 67.8, 34.5.

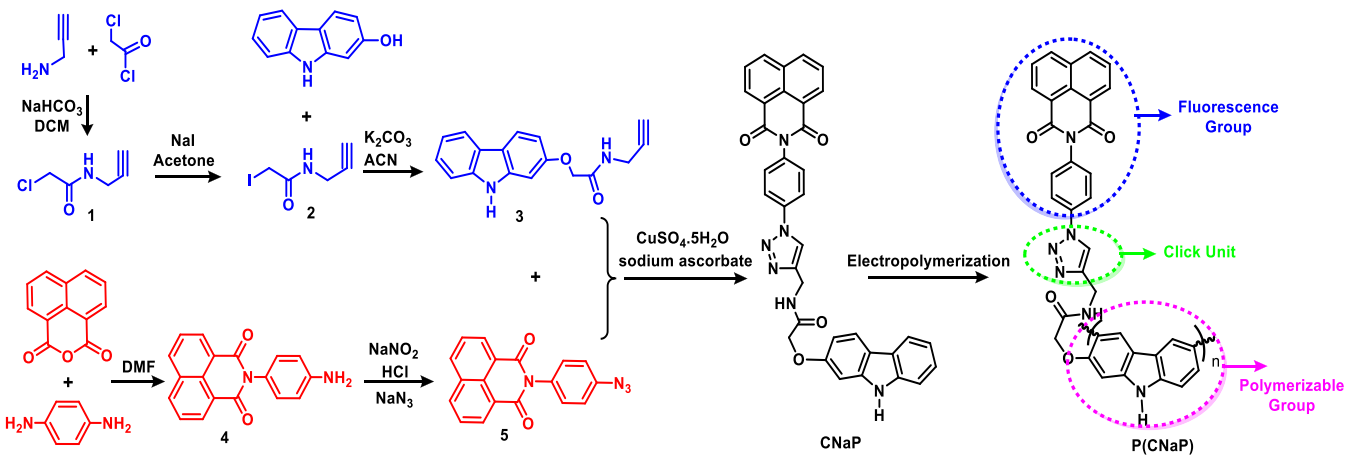

Scheme 1. Synthesis and electropolymerization route of CNaP monomer.

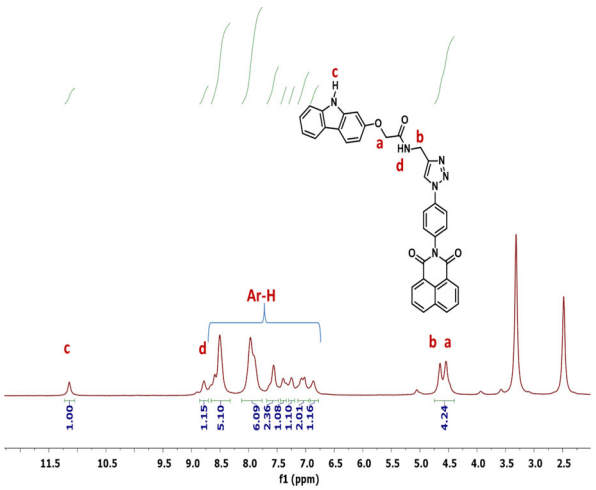

Figure 1. ^{1}H NMR spectrum of CNaP.

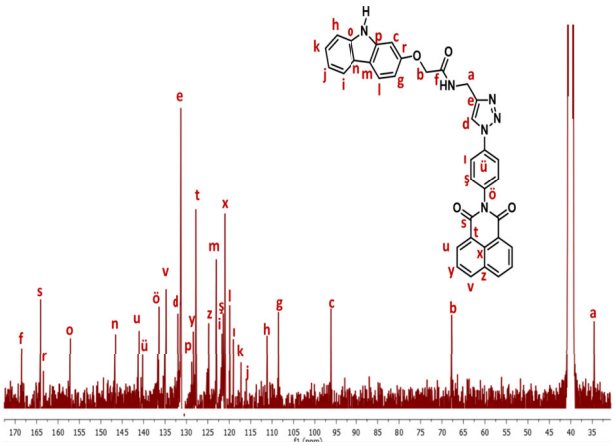

Figure 2. ^{13}C NMR spectrum of CNaP.

Electrochemical polymerization of CNaP

Electrochemical polymerization was performed with an Ivium potentiostat/galvanostat at room temperature. An Ag/Ag^{+} electrode and Pt wire electrode were used as the reference and counter electrode, respectively. Indium tin oxide (ITO) coated glass (dimensions $7 \times 50 \times 0.5$ mm; resistance 8–12 Ω) was used as a working electrode in the three-electrode cell. The PCNaP film was synthesized by electrochemical polymerization on ITO glass in ACN-BFEE (2:1) (v/v) between 0.0 and 1.8 V with a scan rate of 150 mV s^{-1} by cyclic voltammetry (CV). BFEE, a medium strength Lewis acid, can be used in electrochemical polymerization for reducing the onset oxidation potential of electroactive monomers.[47–49] As shown in the literature, BFEE has reduced the resonance energy of carbazole-like electroactive monomers such as thiophene etc.[50–52] Actually CNaP polymerizes in ACN medium but the quality of the film is poor in terms of optical and electrical properties. Furthermore, BFEE was added because it is difficult to form a film of CNaP directly on the electrode in an ACN medium to obtain a high-quality polycarbazole film. The synthesis and electropolymerization route of CNaP monomer are given in Scheme 1.

Spectroelectrochemical and kinetic studies

Spectroelectrochemical studies were performed to investigate the absorption spectra of the resulting PCNaP films upon application of different potentials. The UV spectra were measured using a UV–visible spectrophotometer interfaced with a computer in the three-electrode cell. First, ITO-coated glass without a deposited polymer film was used as the background for spectroelectrochemical measurements. Then, PCNaP polymer films were deposited on ITO by CV between 0 and 1.8 V from a solution of CNaP in ACN-BFEE (2:1) (v/v). UV–visible spectra of the PCNaP polymer films were obtained in monomer-free ACN-BFEE (2:1) (v/v) solution at different potentials.

In kinetic studies, a square wave potential step method was used. In this method, the potential is set to an initial potential value for 5 s; a second potential is then set to the final potential. During this square wave potential step the transmittance (*T*%) and switching times of the polymers were calculated using a UV–visible spectrophotometer.

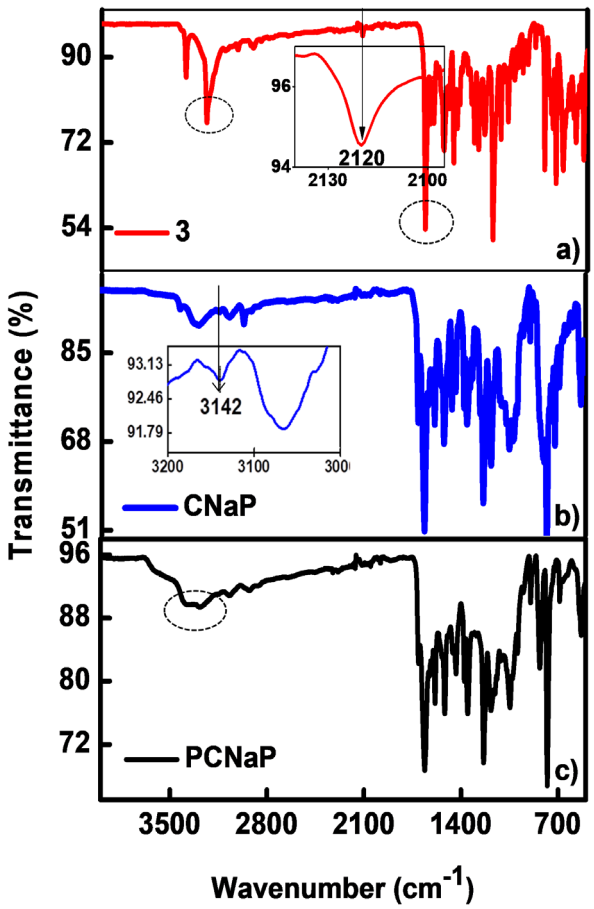

Figure 3. FTIR spectra for (a) molecule **3**; (b) CNaP; (c) PCNaP.

RESULTS AND DISCUSSION

Characterization of the monomer

In the first step, the propargyl derivative of carbazole **3** was synthesized in 81% yield by the reaction of **2** and 2-hydroxycarbazole in the presence of K_2CO_3 in ACN. In the ^{1}H NMR spectrum of **3** there are two resonances for the carbazole amine proton (N—H) at $\delta = 11.13$ ppm and the amide proton at $\delta = 8.89$ ppm that appear as a broad singlet. The peaks at $\delta = 7.97$, 7.37, 7.26, 7.06, 6.96 and 6.80 ppm belong to aromatic protons integrating to a total of seven protons as expected. The peaks at $\delta = 4.56$, 3.91 and 3.07 ppm, respectively, can be assigned to aliphatic protons as a

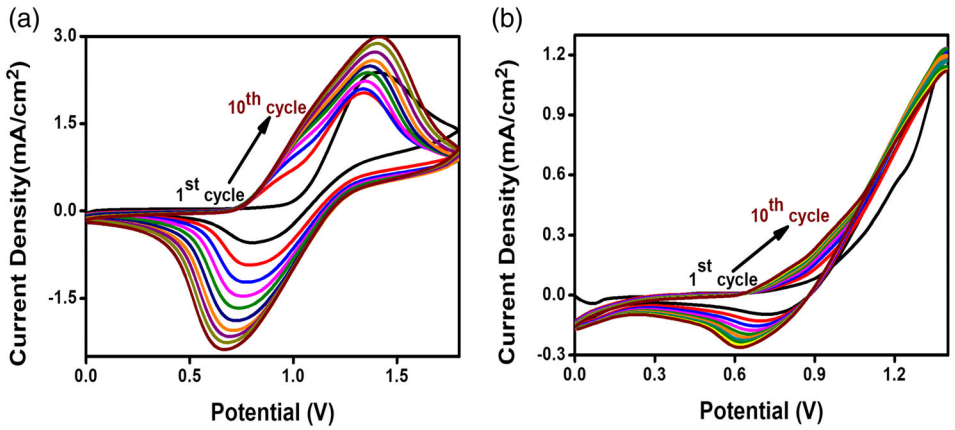

Figure 4. Cyclic voltammograms of (a) CNaP in ACN-BFEE (2:1) (v/v), (b) molecule **3** in ACN-BFEE (2:1) (v/v) at a scan rate of 150 mV s^{-1}.

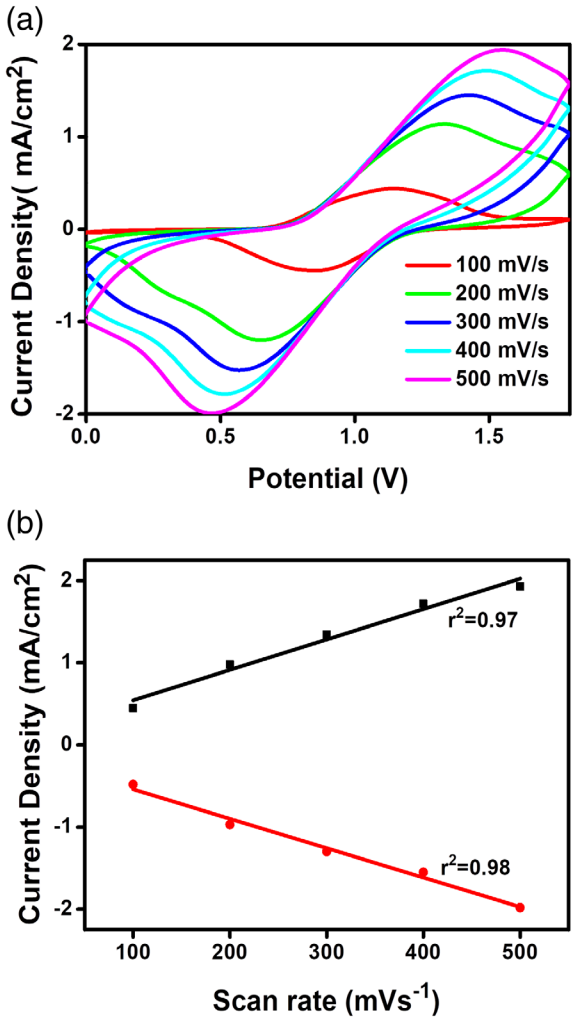

Figure 5. (a) Cyclic voltammograms of PCNaP in ACN-BFEE at different scan rates of 100, 200, 300, 400 and 500 mV s^{-1}. (b) Anodic and cathodic peak current values according to the different scanning rates of PCNaP.

singlet, a doublet and a singlet. In the FTIR spectrum of the propargyl derivative of carbazole, the peaks of the stretching vibrations at 3394, 3243, 2120 and 1667 cm^{-1} represent N—H, C≡CH, C≡C and C═O moieties, respectively. Furthermore, the peaks at 1580 cm^{-1} and 1293 cm^{-1} belong to the C—H bending and C–N stretching vibrations respectively in compound **3**. They also confirm the formation of **3**.

The second step involves the synthesis of naphthalimide azide **5** in 67% yield using naphthalene aminophenyl derivative in the presence of $NaNO_2$ and NaN_3. The ^{1}H NMR spectrum of **5** features aromatic protons belonging to the naphthalene groups as a doublet of doublets (dd) at $\delta = 8.46$ ppm and a triplet at $\delta = 7.87$ ppm. Four protons of the phenyl group appear as a doublet at $\delta = 7.39$ and 7.24 ppm, respectively. The characteristic $-N_3$ stretching peak was observed at 2108 cm^{-1} in the FTIR spectrum, while the amine stretching vibration frequency at 3434 cm^{-1} disappeared. Other stretching and bending vibrations are at 3067 cm^{-1} (aromatic C—H), 1659 cm^{-1} (C═O), 1624 cm^{-1} (N—H bending) and 1234 cm^{-1} (C–N bending).

Lastly, CNaP was synthesized by reacting **3** with **5** via a click reaction in 76% yield. The CNaP was fully characterized by ^{1}H NMR and ^{13}C NMR spectroscopy in DMSO-d_6 as shown in Figs 1 and 2, respectively. These ^{1}H NMR spectral data of CNaP are consistent with the structure proposed based on the observed integrated signal intensity amounting to a total of 24 protons. In the ^{1}H NMR spectrum of CNaP, the aromatic protons belonging to the phenyl group attached to the naphthalimide and carbazole moieties are observed at $\delta = 8.51$, 7.97, 7.39, 7.25, 7.02 and 6.87 ppm and integrate to 18 protons. The proton of the triazole unit appears at $\delta = 7.56$ ppm as a broad singlet. The broad proton resonances at $\delta = 11.14$ ppm and 8.79 ppm belong to carbazole amine proton and amide proton (N—H), respectively. Aliphatic proton signals belonging to the $-OCH_2$ and $-NCH_2$ groups are observed at $\delta = 4.65$ ppm and 4.54 ppm. The ^{13}C NMR spectrum of CNaP indicates that the presence of the triazole unit at $\delta = 131.2$ and 135.0 ppm and aromatic carbon resonances belonging to the naphthalimide and carbazole moieties at $\delta = 163.4–108.5$ integrate to 30 aromatic carbons and can be assigned to amide carbonyl carbon appearing at $\delta = 168.5$ ppm, as displayed in Fig. 2. The signal observed at $\delta = 34.5$ and 67.8 ppm falls into the aliphatic carbon region. As seen from the FTIR spectra graph of the materials (see Fig. 3) the presence of the new stretching vibration at 3142 cm^{-1} belonging to the (C—H) of the triazole unit, absence of the typical azide resonance at 2108 cm^{-1} and disappearance of the propargyl group resonance at 2120 cm^{-1} fully confirm the identity of this compound. In the case of the electrochemically formed polymer of CNaP, shown in Fig. 3(c), the FTIR spectrum observed displays all the characteristic signals of CNaP except that the polymer spectrum resonances are naturally broader.

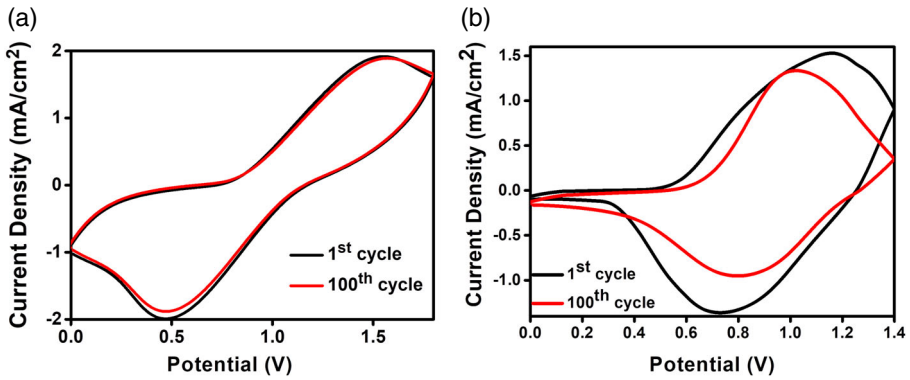

Figure 6. Electrochemical stability via CV with 100 cycles in an ACN-BFEE (2:1) (v/v) solution of (a) PCNaP, (b) poly-3.

Table 1. Electrochemical properties of PCNaP

	λ_{max} (nm)	Switching time (s)	Optical contrast (*T*%)	Stability	E_g (eV)	HOMO (eV)	LUMO (eV)	ΔOD	Qd (mC cm^{-2})	CE (cm^2 C^{-1})
PCNaP	695	1.92	41	95	2.98	−5.16	−2.18	0.63	2.15	181.03

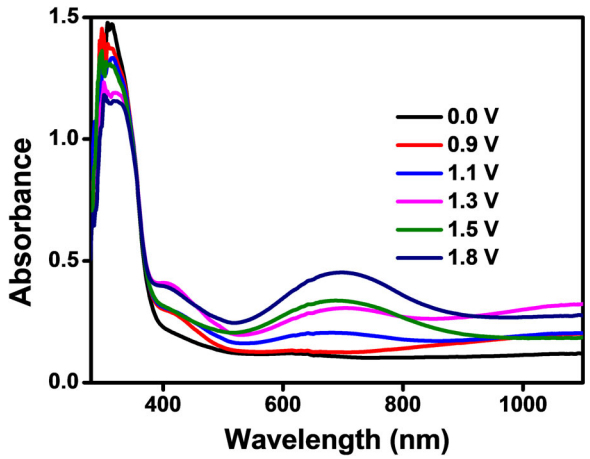

Figure 7. UV–visible absorbance spectra of PCNaP in ACN-BFEE (2:1) (v/v) at various potentials between 0.0 and 1.8 V.

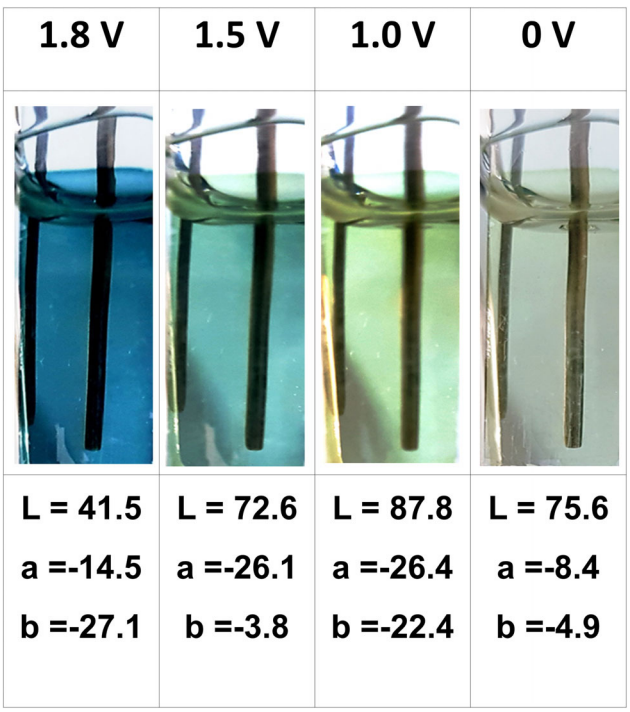

Figure 8. Redox colours of PCNaP.

Electrochemical characterization of PCNaP

CV studies

The electropolymerization of CNaP (1 mmol L^{-1}) was carried out in ACN-BFEE (2:1) (v/v) on the ITO electrode by the CV technique at a scan rate of 150 mV s^{-1}, as shown in Fig. 4(a). The CV graphs of CNaP and molecule **3** are compared. First, as shown in Fig. 4(a), the onset oxidation potential of PCNaP at 0.98 V has appeared at which polymerization begins to form on ITO. The PCNaP film shows a broad oxidation peak between 0.84 and 1.13 V. A reduction peak of PCNaP films was observed at 0.66 V. As shown in Fig. 4(b), the onset potential of molecule **3** was monitored at 0.76 V in the first cycle. The oxidation and reduction potentials of molecule **3** were observed as broad peaks between 0.76 and 0.91 V and at 0.62 V, respectively. A 'poly-3' polymer film was formed on the electrode surface. Binding the carbazole propargyl group to naphthalimide azide via click chemistry caused an increase of 0.22 V in the onset potential. This difference was observed because of the strong electron-withdrawing nature of the naphthalimide group. Moreover, there were certainly differences in the redox potential. Compared to cyclic voltammograms, it was proved by the click reaction that the naphthalimide moieties were bonded to the carbazole compound. Furthermore, as the number of cycles increased, the current density of PCNaP rose, proving that electrochemical polymerization is active on the surface.

Scan rate dependence on PCNaP

PCNaP was subjected to different scan rates from 100 to 500 mV s^{-1} in ACN-BFEE (2:1) (v/v), as seen in Fig. 5. The anodic and cathodic peak current values of the PCNaP film showed a linear increase as a function of the scan rate. This shows that the redox process is

Table 2. Summarized comparison of the electrochemical properties of PCNaP composite films in the literature

Material	λ_{max} (nm)	Switching time (s)	E_g (eV)	Optical contrast (T%)	Stability	CE ($cm^2\ C^{-1}$)	Reference
PCZD	697	2.4	2.59	25	82	NA	60
PETCB	1100	1.6	2.42	36	NA	178.09	61
PTFC	675	1.5	3.07	81	NA	NA	7
PCzRY	660	2.4	3.09	39	84	280	50
PBCBE	570	1.11	2.55	29	NA	NA	62
PED	600	2.0	3.35	36	98	NA	26
PSCZ	762	$t_c = 7.3\ t_b = 1.5$	3.26	61	NA	45	63
PTCP	1075	$t_c = 0.8\ t_b = 0.95$	3.1	NA	80	NA	64
PRDC	700	1.5	2.48	48	91	NA	11
PCNaP	695	1.9	2.98	41	95	181.3	This work

PCZD, poly(9H-carbazol-2-yl-5-(dimethylamino)naphthalene-1-sulfonate); PETCB, poly(ethyl-4-(3,6-di(thiophen-2-yl)-9H-carbazole-9-yl)-benzoate); PTFC, poly(2-(6-((4,6-bis((9H-carbazol-2-yl)oxy)-1,3,5-triazin-2-yl)oxy)-3-oxo-3H-xanthen-9-yl)benzoic acid); PCzRY, poly(sodium(E)-2-((4-((4-((9H-carbazol-2- yl)oxy)-6-((3-((5-carbamoyl-2-hydroxy-1,4-dimethyl-6-oxo-1,6-dihy-dropyridin-3-yl)diazenyl)-4-sulfonatophenyl)amino)-1,3,5-triazin-2-yl) amino)phenyl)sulfonyl)ethyl sulfate]); PBCBE, poly(4-[3,6-bis-(2,3-dihydro-thieno[3,4-b][1,4]dioxin-5-yl)-carbazol-9-yl]-benzoic acid ethyl ester); PED, poly(2,3-dihydrothieno[3,4-b][1,4]dioxin-2-yl)methyl-5-(dimethylamino)naphthalene-1-sulfonate)); PSCZ, poly(2,8-di(carbazol-9-yl) dibenzothiophene); PTCP, poly-1,1,2,2-tetrakis(4-9H-carbazol-9-yl)phenyl)ethane; PRDC, poly((9,9-a-dihydro-4aH-carbazol-2-yl 2- (3,6-bis(diethyl amino)-9H-xanthen-9-yl)benzoate); NA, not available; t_c, time of colouring; t_b, time of bleaching.

not diffusion-controlled and the polymer film adhered well to the electrode surface.[53]

Electrochemical stability of PCNaP

The electrochromic stability of the semiconducting polymers depends on the electrochemical stability because degradation of the active redox couple leads to loss of electrochemical activity. To evaluate the electrochemical stability, the PCNaP and poly-3 were exposed to continuous cycles in monomer-free ACN-BFEE (2:1) (v/v) solution with a scan rate of 500 mV s^{-1}. As shown in Fig. 6(a), the PCNaP film showed a good electrochemical stability of 95% at the end of 100 cycles. In Fig. 6(b), it can be seen that the poly-3 film retains only 73% of its electroactivity after 100 cycles. From that we conclude that the binding of the naphthalimide to the carbazole structure increases the stability of the CNaP polymer in electrochemical redox processes compared to the poly-3 film.

Spectroelectrochemistry of PCNaP

Spectroelectrochemical studies include the use of electrochemical and spectroscopic techniques that are performed simultaneously. PCNaP was electropolymerized on ITO glass by CV between 0 and 1.8 V in the ACN-BFEE (2:1) (v/v) solution system. In neutral form, PCNaP displayed an absorption band centred at 308 nm that is attributed to the $\pi-\pi^*$ transition, as shown in Fig. 7. As the applied potential increased, the absorption band of the $\pi-\pi^*$ transition decreased and bipolaron bands were observed at about 695 nm proving the formation of the polymer chain. The PCNaP film showed transparency in the neutral state (0.0 V) and showed green and blue colours in the oxidized state (Fig. 8). Furthermore, colorimetry detection was performed to find the *L*, *a*, *b* values of the PCNaP films at 1.8 V, 1.5 V, 1.0 V and 0.0 V, respectively, as seen in Fig. 8. The energy of the band gap at the PCNaP film (E_g) was calculated according to the formula $E_g = 1242/\lambda_{onset}$.[54] The optical band gap E_g of PCNaP was obtained from the spectroelectrochemical data by extrapolation using the intersection of the tangent with the *x*-axis from the peak point. The lower energy λ_{onset} of the $\pi-\pi^*$ transition was determined to be 416 nm. E_g was calculated to be 2.98 eV. The highest occupied molecular orbital (HOMO) was calculated to be −5.16 eV according to the equation $E(\text{HOMO}) = -e(\text{Eox}_{onset} + 4.4)$.[55] The lowest unoccupied molecular orbital (LUMO) was derived from the values calculated for the HOMO and the band gap energy (E_g). The result for the LUMO was found to be −2.18 eV according to the equation $E_g = \text{LUMO} - \text{HOMO}$.

The colouring efficiency is defined as the relationship between the injected/removed charge and the change in optical density units as a function of the electrode field. The optical density change (ΔOD) was calculated with the help of the measured transmittance of the PCNaP in the coloured ($T_{coloured}$) and bleached ($T_{bleached}$) state according to the equation

$$\Delta OD = \log(T_{coloured}/T_{bleached})$$

Then, the colouration efficiency (CE) was determined as the ratio of the optical density change (ΔOD) induced and the unit charge density (Qd). It can be calculated using the equation[6,56]

$$\text{CE} = \Delta OD/\text{Qd}$$

Qd (mC cm^{-2}) was calculated using charge–time plots to be 3.48 mC cm^{-2} and the CE value was found to be 181.03 $cm^2\ C^{-1}$. The ideal electrochromic device should show a large change in transmittance with a small increase in charge, giving rise to large colouration efficiency values. The colouration efficiency for inorganic materials was reported to be in the range 10–50 $cm^2\ C^{-1}$. Therefore, the CE value of our PCNaP polymer film (181.03 $cm^2\ C^{-1}$) proves that a semiconducting polymer can be used as a good electrochromic material.

Additionally, PCNaP was deposited on ITO-coated glass to calculate the change in transmittance (*T*%) and the switching time, both of which are important parameters for electrochromic materials. PCNaP was switched between 0.0 and +1.8 V with a switching interval of 5 s in the monomer-free ACN-BFEE (2:1) (v/v) solution system, as shown in Fig. 9(a). The transmittance change value was calculated to be 41% between the neutral state potential (0.0 V) and the oxidized state potential (+1.8 V) at λ_{max} (695 nm).

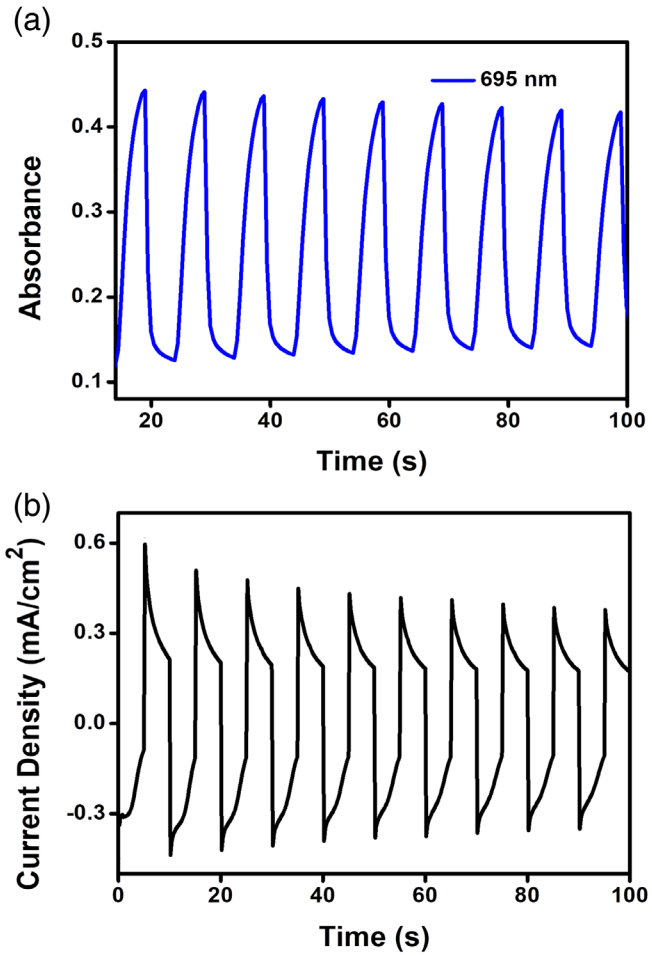

Figure 9. (a) The absorbance and (b) the current density change of CNaP polymer film on applying 0.0 V and 1.8 V.

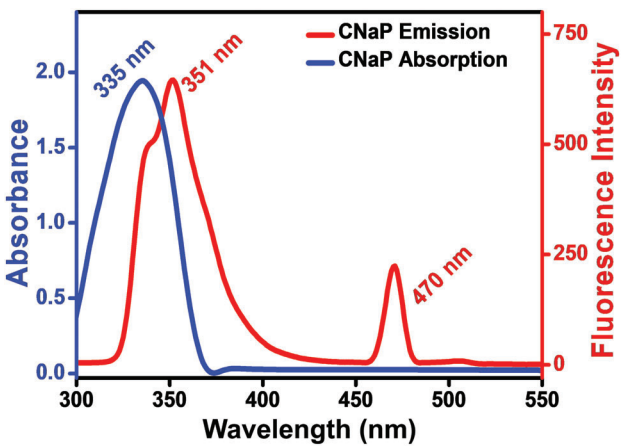

Figure 10. UV–visible and fluorescence spectra of CNaP in ACN solution.

The response time refers to the speed at which an electrochromic polymer switches between its reduced state and oxidized state. The response time was calculated at 90% of the full transmittance change because it is difficult to perceive any further colour change with the naked eye beyond this point.[57] So, 90% of the complete colouring and bleaching were found and the response time was calculated as 1.92 s using this value, as shown in Fig. 9(a).The

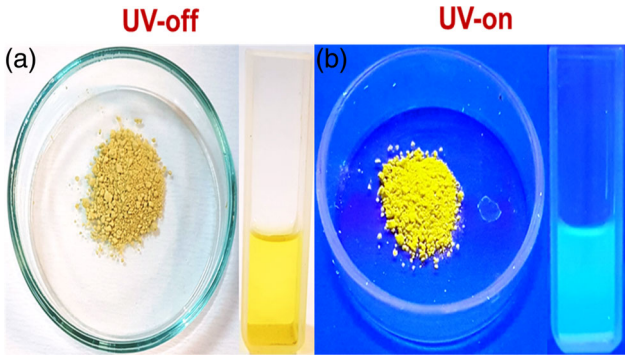

Figure 11. The colour of CNaP (a) in daylight and (b) in UV light.

PCNaP polymer film has moderate response time for large ΔOD, CE and Δ*T*% values at λ_{max} and has good switching stability as it retains almost the entire optical response even after double potential steps. The electrochemical properties of PCNaP are summarized in Table 1.

Fluorescence properties of CNaP

In order to investigate the fluorescence characteristics of the CNaP monomer, UV–visible absorption and fluorescence emission spectra were compared, as shown in Fig. 10. CNaP showed maximum absorbance peaks at 335 nm belonging to $\pi-\pi^*$ transitions; the fluorescence emissions of CNaP demonstrated two characteristic peaks at 351 nm and 470 nm. While the band at 351 nm of CNaP can be attributed to the emission of the carbazole moiety, the band at 470 nm corresponds to the naphthalimide group.[58] Substitution of the cycloaddition ring which is linked by an amino group in naphthalene greatly changes both the absorption and the fluorescence of CNaP. Because of the presence of an emission band at 470 nm, the colour of naphthalimide compounds becomes yellow when naphthalene groups react with the amino group.[59] The new emission peak of CNaP indicates that naphthalimide was attached in the monomer structure via click chemistry. The CNaP monomer in the solid phase displays a light yellow colour in daylight, while it emits a bright yellow colour under UV light. It shows a yellow colour in ACN in daylight and a bright greenish-blue colour when excited with 366 nm UV light (Fig. 11). Thanks to its unique fluorescence properties it can be useful in various fluorescence applications.

In conclusion, Table 2 summarizes a comparison of the electrochemical PCNaP film with related polymers in the literature. The PCNaP film shows moderate optical contrast and large CE values. CE measurements prove that the PCNaP polymer film structure has good electrochromic properties between transparent and green-blue. PCNaP has a moderate switching time indicating that the colour change between the neutral and oxidized state is easy compared to the similar polycarbazole. The electronic energy levels appear at lower energy for some semiconducting polymer films in comparison with PCNaP. This can be explained by the stronger electron-withdrawing nature of the naphthalimide group in the structure of PCNaP.

CONCLUSIONS

In this work, we have successfully designed a functional new fluorescent monomer containing redox-active C (**3**) and fluorescent NaP (**5**) moieties synthesized by Cu-catalyzed click chemistry. After

electropolymerization, the electrochromic and spectroelectrochemical properties of PCNaP were determined. The polymer films demonstrated moderate stability (95%) and optical contrast of 41%. The CNaP monomer possesses a bright greenish-blue colour in ACN when excited with 366 UV light. The fluorescence emission of CNaP at 470 nm indicates that the naphthalimide was successfully attached to CNaP via the click protocol. The conductive polymer film (PCNaP) obtained from the fluorescent monomer was shown to possess the potential for use in electrochromic devices.

ACKNOWLEDGEMENTS

This research was financially supported by PAU-BAP (2018FEBE020) and the BAGEP Award of the Science Academy.

DECLARATIONS OF INTEREST

None.

DATA AVAILABILITY

The raw/processed data required to reproduce these findings cannot be shared at this time due to technical or time limitations.

REFERENCES

1 Gumusay O, Soganci T, Soyleyici HC, Ak M and Cetisli H, *J Electrochem Soc* **164**:H421–H429 (2017). https://doi.org/10.1149/2.0291707jes.
2 Ribeiro AS and Mortimer RJ, *SPR Electrochem* **13**:21–49 (2016). https://doi.org/10.1039/9781782620273-00021.
3 Park J-S, Chae H, Chung HK and Lee SI, *Semicond Sci Technol* **26**:034001 (2011). https://doi.org/10.1088/0268-1242/26/3/034001.
4 Camurlu P and Karagoren N, *React Funct Polym* **73**:847–853 (2013). https://doi.org/10.1016/j.reactfunctpolym.2013.03.014.
5 Ayranci R, Ak M, Ocal S and Karakus M, *Des Monomers Polym* **19**:429–436 (2016). https://doi.org/10.1080/15685551.2016.1169377.
6 Ayranci R, Başkaya G, Güzel M, Bozkurt S, Şen F and Ak M, *ChemistrySelect* **2**:1548–1555 (2017). https://doi.org/10.1002/slct.201601632.
7 Guzel M, Karatas E and Ak M, *J Electrochem Soc* **165**:H437–H445 (2018). https://doi.org/10.1149/2.0521809jes.
8 Mortimer RJ, Dyer AL and Reynolds JR, *Displays* **27**:2–18 (2006). https://doi.org/10.1016/j.displa.2005.03.003.
9 Erlik O, Unlu NA, Hizalan G, Hacioglu SO, Comez S, Yildiz ED *et al.*, *J Polym Sci A Polym Chem* **53**:1541–1547 (2015). https://doi.org/10.1002/pola.27625.
10 Österholm AM, Shen DE, Kerszulis JA, Bulloch RH, Kuepfert M, Dyer AL *et al.*, *ACS Appl Mater Interfaces* **7**:1413–1421 (2015). https://doi.org/10.1021/am507063d.
11 Ayranci R and Ak M, *J Electrochem Soc* **164**:H509–H514 (2017). https://doi.org/10.1149/2.0281707jes.
12 Oyman G, Geyik C, Ayranci R, Ak M, Odaci Demirkol D, Timur S *et al.*, *RSC Adv* **4**:53411–53418 (2014). https://doi.org/10.1039/C4RA08481K.
13 Kirankumar R, Huang W-C, Chen H-F and Chen P-Y, *J Electroanal Chem* **826**:198–206 (2018). https://doi.org/10.1016/j.jelechem.2018.08.043.
14 Soganci T, Baygu Y, Kabay N, Gök Y and Ak M, *ACS Appl Mater Interfaces* **10**:21654–21665 (2018). https://doi.org/10.1021/acsami.8b06206.
15 Olgac R, Soganci T, Baygu Y, Gök Y and Ak M, *Biosens Bioelectron* **98**:202–209 (2017). https://doi.org/10.1016/j.bios.2017.06.028.
16 Soganci T, Ayranci R, Harputlu E, Ocakoglu K, Acet M, Farle M *et al.*, *Sens Actuators B* **273**:1501–1507 (2018). https://doi.org/10.1016/j.snb.2018.07.064.
17 Ayranci R, Torlak Y, Soganci T and Ak M, *J Electrochem Soc* **165**:B638–B643 (2018). https://doi.org/10.1149/2.1061813jes.
18 Ayranci R, Kirbay FO, Demirkol DO, Ak M and Timur S, *Methods Appl Fluoresc* **6**:035012 (2018). https://doi.org/10.1088/2050-6120/aac519.
19 Ayranci R, Demirkol D, Ak M and Timur S, *Sensors* **15**:1389–1403 (2015). https://doi.org/10.3390/s150101389.
20 Beaupré S, Breton A-C, Dumas J and Leclerc M, *Chem Mater* **21**:1504–1513 (2009). https://doi.org/10.1021/cm802941e.
21 Lelii C, Bawendi MG, Biagini P, Chen P-Y, Crucianelli M, J.M. D'Arcy F *et al.*, *J Mater Chem A* **2**:18375–18382 (2014). https://doi.org/10.1039/C4TA03098B.
22 P.M. Beaujuge, J. Subbiah, K.R. Choudhury, S. Ellinger, T.D. Mccarley, F. So, J.R. Reynolds, *Chem Mater* **22**:2093–2106 (2010). https://doi.org/10.1021/cm903495b.
23 Unlu NA, Hacioglu SO, Hizalan G, Yildiz DE, Toppare L and Cirpan A, *J Electrochem Soc* **164**:G71–G76 (2017). https://doi.org/10.1149/2.0201707jes.
24 Xu C, Zhao J, Wang M, Wang Z, Cui C, Kong Y *et al.*, *Electrochim Acta* **75**:28–34 (2012). https://doi.org/10.1016/j.electacta.2012.04.159.
25 Zhu X, Xu L, Wang M, Wang Z, Liu R and Zhao J, *Int J Electrochem Sci* **6**:1730–1746 (2011).
26 Ayranci R and Ak M, *J Electrochem Soc* **164**:H925–H930 (2017). https://doi.org/10.1149/2.1621713jes.
27 Koyuncu FB, Koyuncu S and Ozdemir E, *Electrochim Acta* **55**:4935–4941 (2010). https://doi.org/10.1016/j.electacta.2010.03.094.
28 Michinobu T, Osako H and Shigehara K, *Polymers (Basel)* **2**:159–173 (2010). https://doi.org/10.3390/polym2030159.
29 Morin J-F and Leclerc M, *Macromolecules* **34**:4680–4682 (2001). https://doi.org/10.1021/ma010152u.
30 Blouin N and Leclerc M, *Acc Chem Res* **41**:1110–1119 (2008). https://doi.org/10.1021/ar800057k.
31 Bekere L, Gachet D, Lokshin V, Marine W and Khodorkovsky V, *Beilstein J Org Chem* **9**:1311–1318 (2013). https://doi.org/10.3762/bjoc.9.147.
32 Li-Ping Z, Wan-Dong C and Rui-Fa J, *Org Chem Curr Res* **04**:1–5 (2014). https://doi.org/10.4172/2161-0401.1000134.
33 Bardajee GR, Li AY, Haley JC and Winnik MA, *Dye Pigment* **79**:24–32 (2008). https://doi.org/10.1016/j.dyepig.2007.12.012.
34 Zhang W, Xu Y, Hanif M, Zhang S, Zhou J, Hu D *et al.*, *J Phys Chem C* **121**:23218–23223 (2017). https://doi.org/10.1021/acs.jpcc.7b07513.
35 Xuhong Q, Jim T, Jiandong Z and Yulan Z, *Dye Pigment* **25**:109–114 (1994). https://doi.org/10.1016/0143-7208(94)85042-9.
36 Han SC, Choi I-H, Jin S-H and Lee JW, *Mol Cryst Liq Cryst* **599**:86–95 (2014). https://doi.org/10.1080/15421406.2014.935969.
37 Li H, Sun J, Qin A and Tang BZ, *Chinese J Polym Sci* **30**:1–15 (2012). https://doi.org/10.1007/s10118-012-1098-2.
38 Carlmark A, Hawker C, Hult A and Malkoch M, *Chem Soc Rev* **38**:352–362 (2009). https://doi.org/10.1039/B711745K.
39 Hein JE and Fokin VV, *Chem Soc Rev* **39**:1302–1315 (2010). https://doi.org/10.1039/b904091a.
40 Fu R and Fu G-D, *Polym Chem* **2**:465–475 (2011). https://doi.org/10.1039/C0PY00174K.
41 Thirumurugan P, Matosiuk D and Jozwiak K, *Chem Rev* **113**:4905–4979 (2013). https://doi.org/10.1021/cr200409f.
42 Binder WH and Sachsenhofer R, *Macromol Rapid Commun* **28**:15–54 (2007). https://doi.org/10.1002/marc.200600625.
43 Sumerlin BS and Vogt AP, *Macromolecules* **43**:1–13 (2010). https://doi.org/10.1021/ma901447e.
44 Hvilsted S, *Polym Int* **61**:485–494 (2012). https://doi.org/10.1002/pi.4135.
45 Milne M, Chicas K, Li A, Bartha R and Hudson RHE, *Org Biomol Chem* **10**:287–292 (2012). https://doi.org/10.1039/C1OB06162C.
46 Jian F-F, Wang L-M, Du L and Wang J, *Acta Crystallogr Sect E Struct Rep Online* **64**:o263–o263 (2008). https://doi.org/10.1107/S160053680706583X.
47 Shi G, Li C and Liang Y, *Adv Mater* **11**:1145–1146 (1999). https://doi.org/10.1002/(SICI)1521-4095(199909)11:13<1145::AID-ADMA1145>3.0.CO;2-T.
48 Nie G, Yang H, Wang S and Li X, *Crit Rev Solid State Mater Sci* **36**:209–228 (2011). https://doi.org/10.1080/10408436.2011.593009.
49 Soyleyici S, Karakus M and Ak M, *J Electrochem Soc* **163**:H679–H683 (2016). https://doi.org/10.1149/2.0711608jes.
50 Guzel M and Ak M, *Org Electron* **75**:105436 (2019). https://doi.org/10.1016/j.orgel.2019.105436.
51 Guzel M, Soganci T, Akgun M and Ak M, *J Electrochem Soc* **162**:H527–H534 (2015). https://doi.org/10.1149/2.0651508jes.
52 Ak M and Soganci T, Electrochemical properties and electrochromic device applicationsof polycarbazole derivatives, In: Xu JW, Chua MH, Kwok Wei Shah KW (ed). Electrochromic Smart Materials Fabrication and Applications, London: Royal Society of Chemistry, 293–322 (2019). https://doi.org/10.1039/9781788016667-00293

53 Kumar A, Welsh DM, Morvant MC, Piroux F, Abboud KA and Reynolds JR, *Chem Mater* **10**:896–902 (1998). https://doi.org/10.1021/cm9706614.
54 Udum YA, Hızlıateş CG, Ergün Y and Toppare L, *Thin Solid Films* **595**:61–67 (2015). https://doi.org/10.1016/j.tsf.2015.10.055.
55 Brbdas JL, Silbey R, Boudreaux DS and Chance RR, Chain-length dependence of electronic and electrochemical properties. **105**:6555–6559 (1983).
56 Ayranci R, Baskaya G, Guzel M, Bozkurt S, Ak M, Savk A *et al.*, *Nano-Struct Nano-Objects* **11**:13–19 (2017). https://doi.org/10.1016/j.nanoso.2017.05.008.
57 Hsiao SH and Lin SW, *Polym Chem* **7**:198–211 (2016). https://doi.org/10.1039/c5py01407g.
58 Kukhta A, Kolesnik E, Grabchev I and Sali S, *J Fluoresc* **16**:375–378 (2006). https://doi.org/10.1007/s10895-005-0064-6.
59 Alexiou MS, Tychopoulos V, Ghorbanian S, Tyman JHP, Brown RG and Brittain PI, *J Chem Soc, Perkin Trans* **2**:837–842 (1990). https://doi.org/10.1039/P29900000837.
60 Ayranci R, Vargün E and Ak M, *ECS J Solid State Sci Technol* **6**:P211–P216 (2017). https://doi.org/10.1149/2.0061705jss.
61 Hu B, Lv X, Sun J, Bian G, Ouyang M, Fu Z *et al.*, *Org Electron Physics, Mater Appl* **14**:1521–1530 (2013). https://doi.org/10.1016/j.orgel.2013.03.024.
62 Hu B, Zhang X, Liu J, Chen X, Zhao J and Jin L, *Synth Met* **228**:70–78 (2017). https://doi.org/10.1016/j.synthmet.2017.04.011.
63 Hsiao S and Wu L, *Dye Pigment* **134**:51–63 (2016). https://doi.org/10.1016/j.dyepig.2016.06.043.
64 Carbas C, B B, Odabas S and Türksoy F, *Electrochim Acta* **193**:72–79 (2016). https://doi.org/10.1016/j.electacta.2016.02.024.

